Am J Transl Res 2024;16(8):3950-3963
www.ajtr.org /ISSN:1943-8141/AJTR0157474

Original Article

Identification of RAS-like oncoprotein B (RALB) as a potential prognostic and therapeutic target in head and neck squamous cell carcinoma

Zi-Yuan Zhou[1,2], Lei Liu[3], Xiao-Meng Song[1,2]

[1]Department of Oral and Maxillofacial Surgery, Affiliated Hospital of Stomatology, Nanjing Medical University, Nanjing, Jiangsu, China; [2]Jiangsu Key Laboratory of Oral Diseases, Jiangsu Province Engineering Research Center of Stomatological Translational Medicine, Nanjing Medical University, Nanjing, Jiangsu, China; [3]Department of Orthopedics, The Affiliated Yixing Hospital of Jiangsu University, Yixing, Jiangsu, China

Received April 28, 2024; Accepted July 1, 2024; Epub August 15, 2024; Published August 30, 2024

Abstract: Background/purpose: The RAS superfamily oncogenes play significant roles in various types of malignant tumors. However, little is known about the role of RAS-like oncoprotein B (RALB) in head and neck squamous cell carcinoma (HNSCC). This study evaluated whether RALB can be a prognostic and therapeutic target for HNSCC. Materials and methods: A total of 504 HNSCC samples from The Cancer Genome Atlas database were segregated into two groups: RALB-high and RALB-low. The clinical significance of RALB expression in HNSCC patients was investigated. Cell proliferation, migration, and invasion assays were performed in HN-1 and HN-5 cells by silencing RALB using siRNA. Gene enrichment and immune infiltration analyses were also performed. Results: RALB expression was elevated in HNSCC tissues compared with normal tissues and was an independent risk factor associated with poor prognosis. A nomogram including the RALB expression level was established to predict the prognosis of HNSCC patients and showed highest sensitivity and benefit in predicting the three-year survival. The inhibition of RALB expression effectively impeded the proliferation, invasion, and migration of HNSCC cells. Importantly, RALB levels were significantly correlated with T cell-mediated immune responses, especially in human papillomavirus-positive HNSCC samples. Conclusion: This study identified RALB as a potential prognostic and therapeutic target for HNSCC, and provided insight into the relationship between RALB and revealed an innovative strategy for HNSCC immunotherapy.

Keywords: Head and neck cancer, immunotherapy, RAL GTPases, RAS-like oncoprotein, survival

Introduction

Head and neck squamous cell carcinoma (HNSCC) is one of the most common types of cancer, and is a leading cause of cancer death worldwide [1]. Despite advances in surgery, radiotherapy, and chemotherapy, the 5-year survival rate of HNSCC patients has been at approximately 50% over the past decades [2]. The prognosis of HNSCC patients, especially those at the advanced-stage, remains poor due to recurrence and metastasis. The current approach of prognosis prediction focuses on patients' clinical manifestations, such as the location of the tumor, pathological classification, metastasis status, and sensitivity to chemotherapy [3]. However, HNSCC patients with different molecular types may have similar clinical manifestations before and during treatment, they therefore often have different outcomes of prognosis [4, 5]. Further exploration of the etiological mechanisms of HNSCC and identification of novel treatment targets are urgently needed, so as to develop more effective treatment strategies for HNSCC and to improve patient outcomes. Understanding new molecular events involved in the development and progression of HNSCC may help to develop new drug targets and biomarkers, not only for early diagnosis but also for personalized treatment plans based on genetic and epigenetic alterations [6-9].

RAS-like oncoprotein B (RALB) is a small GTPase that is a critical to the downstream effectors of the RAS superfamily [10]. Mutations in the

https://doi.org/10.62347/NDFC4209

three RAS oncogenes (HRAS, NRAS, and KRAS) occur in approximately 32% of all human cancers [11]. Unlike many of the other RAS superfamily members, the structure of RAL is amenable to drug targeting. Research on RAL GTPases in cancer continues to clarify (do not understand why use "clarify") their important roles in many cancer subtypes and reinforce their attractiveness as therapeutic targets [12]. Most evidence have indicated that RALB is required for the survival of malignant but not normal cells, making it an attractive therapeutic target [13]. Additionally, RALB is important for the progression and metastasis of bladder and lung cancers [12]. Research on RALB in cancer continues to clarify its essential roles in many cancer subtypes and reinforce its attractiveness as a therapeutic target (repeat, should be deleted). Moreover, multiple studies have shown that RAL GTPases can be used as effective markers for predicting the prognosis of patients with tumors such as osteosarcoma, non-small cell lung cancer, and colon cancer [14-16].

However, whether RALB signaling downstream of RAS and has a role in HNSCC is largely unknown [12]. Understanding how the dysregulation of RALB in HNSCC maintains invasion and metastasis is a critical step toward development of effective RAS targeted treatment strategies. Therefore, this study was conducted to elucidate the dysregulation of RALB in HNSCC and to evaluate its potential as a prognostic biomarker for patient survival and as a therapeutic target. This study provides novel insights into the prospects of targeting RALB in immunotherapy for HNSCC.

Materials and methods

Public data resources and data processing

Raw public data were obtained from The Cancer Genome Atlas (TCGA, *https://portal.gdc.cancer.gov/*) and the TIMER dataset (*https://cistrome.shinyapp-s.io/timer/*). HNSCC patient information was collected exclusively from the TCGA and normal tissue information was obtained from the GteX database. Immunization-related information was retrieved solely from TIMER. A total of 504 HNSCC patients from the TCGA database were segregated into two groups according to their RALB mRNA expression levels, namely, the RALB-high and RALB-low groups, utilizing the median value as a threshold. The differentially expressed genes (DEGs) between the two groups were analyzed using the DESeq2 package. DEGs with a log2-fold change greater than or equal to 1 and an adjusted *p*-value less than 0.05 were considered to be significantly differentially expressed. Enrichment analysis of DEGs was performed with Kyoto Encyclopedia of Genes (KEGG) using the clusterProfiler R package, and the org.Hs.eg.db R package was used to assess the functional enrichment.

Patient tissue samples and immunohistochemistry (IHC)

The Ninety (90) patients from the Department of Stomatology, Affiliated Hospital of Nanjing Medical University were included in the clinical study. The Ethics Committee of the Affiliated Hospital of Nanjing Medical University approved the experimental protocol. All study participants signed informed consent forms. The clinical patients' inclusion criteria and baseline data are described in detail in the supplementary materials (Table S4).

The inclusion criteria for HNSCC patients in this study were as follows: (1) The primary HNSCC's main treatment modality was surgical resection, and no neoadjuvant therapy (radiation therapy or chemotherapy, etc.) was administered before surgery. (2) Human papillomavirus (HPV) status was confirmed to be negative. (3) Paraffin-embedded tissues had sufficient invasive margins and tumor center regions for subsequent analysis. The IHC analysis in tissue microarray in this study were performed following a standard protocol.

Cell line and culture

The HNSCC cell lines HN-1 and HN-5 were acquired from the Cell Bank of Type Culture Collection of the Chinese Academy of Sciences, Shanghai, China, and cultured in DMEM medium supplemented with 10% fetal bovine serum (FBS; Thermo Fisher Scientific Inc., Waltham, MA, USA). The cells were maintained at 37°C in an environment containing 5% CO_2.

Cell transfection

Plasmids encoding the human RALB open reading frame (ORF) were obtained from GenScript

(GenScript Inc., Shanghai, China) and used for transfection of HNSCC cells with Lipofectamine 3000® reagent (Thermo Fisher Scientific Inc.). An empty vector was used as a control. Cells were harvested either after 24 hours of transfection or when the cells reached maximum confluence. Table S1 contains the sequences of the siRNAs and control plasmids.

Cell proliferation assay

The proliferation of HNSCC cells was assessed using a Cell Proliferation Assay kit that incorporated 5-ethynyl-2'-deoxyuridine (EdU), following the manufacturer's instructions (Takara Bio. Inc., Beijing, China). The data obtained were analyzed using the Image Pro Plus software version 7.0 (Media Cybernetics Inc.).

Cell migration assay

The migratory ability of HNSCC cells was assessed by performing a wound healing assay, where the treated cells (at 100% confluence) were cultured in 6-well cell culture plates and subjected to scraping with the tip of a 200 µl pipette. Wound closure was monitored by imaging with a photomicroscope (Olympus Corporation; model: BX51; Olympus Co., Tokyo, Japan) at 0 and 24 hours, following incubation in serum-free medium.

Cell invasion assay

The invasive capacity of HNSCC cells was assessed using 12-well Millicell cell culture inserts. After transfection, HNSCC cells suspended in a DMEM medium supplemented with 1% FBS were added to the top chamber. DMEM supplemented with 10% FBS was added to each well. Following a 20-hour incubation period under a humidified atmosphere containing 5% CO_2, HNSCC cells could migrate and infiltrate through gelatin-coated polycarbonate membranes toward the bottom chamber where more nutritious DMEM supplemented with higher levels of FBS was present. Subsequently, the cells on the outer surface of each insert were rinsed and then fixed at room temperature using a paraformaldehyde solution (Sangon Biotech Co., Shanghai, China) protected from light. The cells were then stained with purple crystals (Sangon Biotech Co.) and observed using a photomicroscope (BX51; Olympus Co.). Five fields of view were randomly selected for analysis.

Reverse transcription-quantitative PCR (RT-qPCR)

Total RNA was extracted from cells and tissue samples for further study using TRIzol® reagent (Thermo Fisher Scientific Inc.). The RNA concentration was measured using a microplate reader. To quantify RALB mRNA expression levels, we reverse transcribed 1 µg of total RNA into cDNA using avian myeloblastic virus reverse transcriptase and Oligo(dT) primers (Takara Bio. Inc.). The reaction mixture was incubated: at 16°C for 5 min, 42°C for 60 min, and 70°C for 10 min. Then, the RT-qPCR mixture, which consisted of specific primers for RALB and GAPDH and SYBR Green dye (Thermo Fisher Scientific Inc.), was incubated under the following conditions: 95°C for 5 min, followed by 40 cycles of 95°C for 30 s, 60°C for 30 s, and 72°C for 1 min. All primer sequences are presented in Table S2. The expression levels were quantified using the $2^{-\Delta\Delta Cq}$ method and normalized to the expression of GAPDH.

Immune infiltration analysis

TIMER was used to systematically evaluate the infiltration of various immune cells and their clinical impacts [17]. In this study, we analyzed the correlation between tumor purity and tumor-infiltrating immune cells with the TIMER Gene and Correlation modules. The "ssGSEA" "ESTIMATES" R package was used to analyze the profiles of tumor-infiltrating immune cells in HNSCC patients and the differentially infiltrated immune cells between the two patient groups. The "ESTIMATES" R package was used to evaluate the correlation between stromal and immune infiltration levels and RALB levels in HNSCC patients.

Statistical analysis

Data from cell proliferation, migration, and invasion assays, together with the animal experiments, are representative of at least three independent experiments. All sample data were analyzed using SPSS software (version 11.0, SPSS, IBM SPSS, Madrid, España). RT-qPCR and dual luciferase reporter assays were performed in triplicate. The data are presented as the mean ± SEM. Pearson coefficient is used for correlation analysis. Two-group comparisons were calculated by Student's t-test. $P<0.05$ was considered to indicate a significant

difference. All the statistical analyses and |visualizations of clinically relevant data and sequencing results were conducted in R (version 3.6.3).

Results

RALB protein and mRNA expression are increased in HNSCC

The expression levels of RAS-related genes in HNSCC were determined. The combined analysis of the TCGA database and GteX databases revealed that the mRNA expression levels of RAS subtypes (HRAS, NRAS, and KRAS) in HNSCC tissues were significantly greater than those in normal tissues (**Figure 1A**). Importantly, there was a significant positive correlation between RALB expression level and NRAS/KRAS in HNSCC tissues. However, such correlation was not found with HRAS (**Figure 1B**). We examined the expression level of RALB, as a vital molecule downstream of the RAS, in HNSCC and its correlation with survival-related indicators (overall survival (OS), disease-specific survival (DSS), and recurrence-free interval (RFI)) in HNSCC patients to determine whether RALB participates in the malignant behavior of HNSCC (Table S3). As shown in **Figure 1C** and **1D**, both the paired and unpaired expression differences indicated that the mRNA level of RALB in HNSCC tissues was greater than that in normal tissues. Furthermore, patients with HNSCC with high levels of RALB expression had a significantly worse prognosis than those with low levels of RALB expression (**Figure 1E**).

RALB expression is upregulated in HNSCC clinical samples

To further validate the expression level of RALB in HNSCC patients, we employed immunohistochemistry to measure the expression level of RALB in clinical samples from 90 HNSCC patients, with 20 normal mucosal tissue samples serving as the control group. The results demonstrated a significantly greater level of RALB protein in HNSCC tissues than in normal mucosal tissues (**Figure 2A** and **2B**). According to the Kaplan-Meier survival analysis and log-rank tests, HNSCC patients with high RALB expression exhibited lower OS rates (P=0.017, **Figure 2C**). RT-qPCR results also revealed significantly greater levels of the RALB mRNA in the tumor tissues of fresh HNSCC patients than in the adjacent normal tissues (**Figure 2D**). Furthermore, we investigated the relationship between the RALB expression level in HNSCC tissues and the corresponding patient clinicopathological characteristics (Table S4). By classifying the expression of RALB in the 90 HNSCC tissues according the median IHC score, we found a significant positive correlation between RALB expression and lymph node metastasis (**Figure 2E**). Taken together, the results of these clinical studies demonstrated elevated expression levels of RALB in HNSCC tissues compared to those in adjacent normal tissues. Furthermore, HNSCC patients with high RALB expression are more prone to metastasis and exhibit lower OS rates.

RALB upregulation is a valuable prognostic marker for HNSCC patients

Given the strong correlation between RALB and the prognosis of HNSCC patients, incorporating RALB as a marker into the HNSCC prognosis prediction system was expected to yield considerable benefits for patients. Multivariate Cox proportional hazards regression analysis revealed that the RALB expression level and N stage were significant factors affecting the prognosis of HNSCC patients (P<0.05) (Table S5). To integrate the significant impact of the RALB expression level on HNSCC patients' prognosis into the prognostic evaluation system, a nomogram for HNSCC prognostic risk was constructed according to the multivariate Cox regression results. The nomogram includes a scoring scale to assess the risk factors for HNSCC patients, which can be used to calculate survival risks at 1, 3, and 5 years (**Figure 3A**). The correlations between RALB and other risk factors are illustrated in **Figure 3B**. Additionally, receiver operating characteristic (ROC) curves were generated to evaluate the sensitivity of the RALB level as a predictive marker for HNSCC prognosis. We utilized the Calibration curve to assess the advantages of incorporating RALB levels into the prognostic prediction system for HNSCC patients in contrast to conventional clinical programs at various time intervals. As anticipated, the RALB level demonstrated significant sensitivity and relatively high efficacy as a prognostic indicator for HNSCC (**Figure 3C** and **3E**). Additionally, we employed a time-dependent Area Under Curve (AUC) to gauge the sensitivity of our prognostic

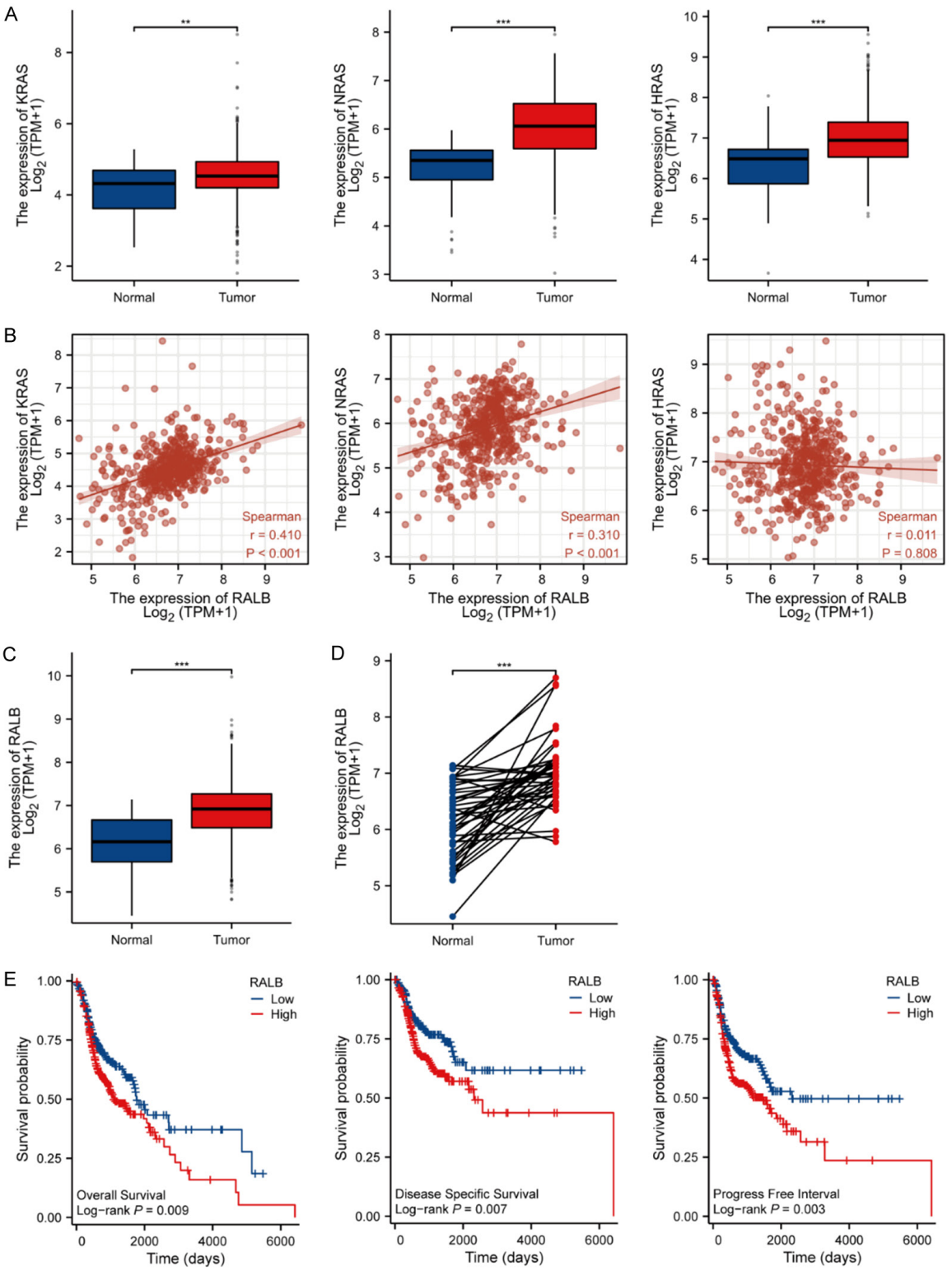

Figure 1. RALB is highly expressed and related to worse prognosis in HNSCC. A. mRNA level of KRAS, NRAS, and HRAS in HNSCC samples from the TCGA database and normal tissue samples from the GTeX database. B. Correlation between RALB mRNA level and KRAS, NRAS, and HRAS mRNA level in HNSCC samples from the TCGA database. C. mRNA level of RALB in HNSCC samples from the TCGA database and normal tissue samples from the GTeX database. D. mRNA level of RALB of paired HNSCC samples and normal tissue samples from the TCGA database. E. Overall survival (OS), disease-specific survival (DSS), and progress-free survival (PFS) of HNSCC patients satisfied by RALB level using Kaplan-Meier analyses. **, P<0.01; ***, P<0.001.

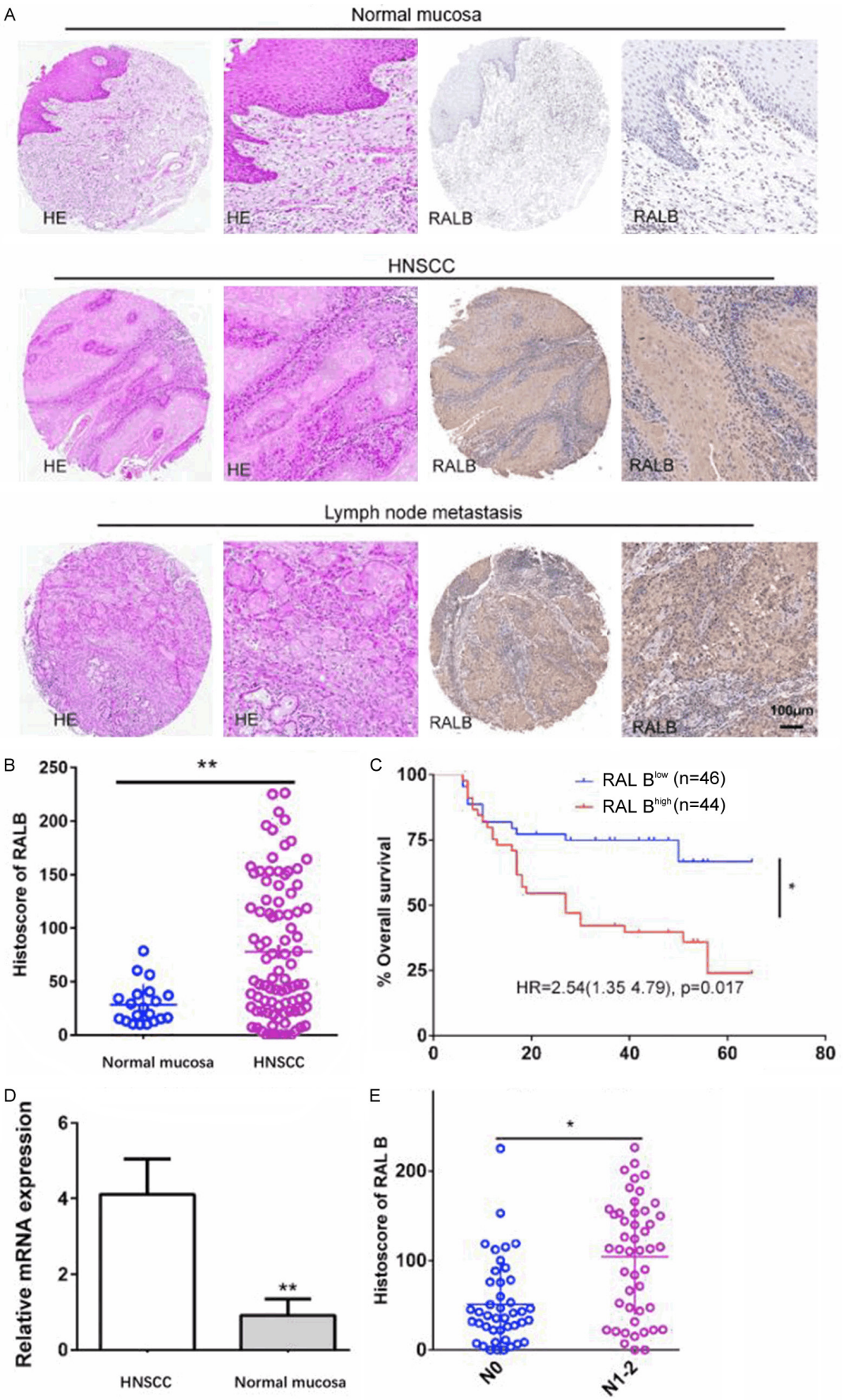
A
Normal mucosa
HE
HE
RALB
RALB
HNSCC
HE
HE
RALB
RALB
Lymph node metastasis
HE
HE
RALB
RALB
100μm
B
Histoscore of RALB
250
200
150
100
50
0
**
Normal mucosa
HNSCC
C
% Overall survival
100
75
50
25
0
RAL B^low (n=46)
RAL B^high (n=44)
*
HR=2.54(1.35 4.79), p=0.017
0
20
40
60
80
D
Relative mRNA expression
6
4
2
0
**
HNSCC
Normal mucosa
E
Histoscore of RAL B
200
100
0
*
N0
N1-2

Figure 2. High expression of RALB in clinical samples of HNSCC positively correlates with lymph node metastasis and poor prognosis. A. Expression of RALB in normal mucosa (top), HNSCC (middle), and HNSCC lymph node metastasis specimens (bottom) shown by H&E staining and immunohistochemical staining, scale bar =100 μm. B. Immunohistochemical scoring reveals significantly higher expression of RALB in HNSCC tissues (n=88) compared to normal mucosa tissues (n=20). C. Overall survival of HNSCC patients stratified by RALB level using Kaplan-Meier analysis. *, P<0.05. D. Relative levels of RALB mRNA in fresh paired tumor tissues of HNSCC patients and normal tissues assessed by RT-qPCR. E. Immunohistochemical scoring analysis of RALB expression levels in HNSCC patients with lymph node metastasis (N+, n=47) and without lymph node metastasis (N0, n=41). **, *P*<0.01.

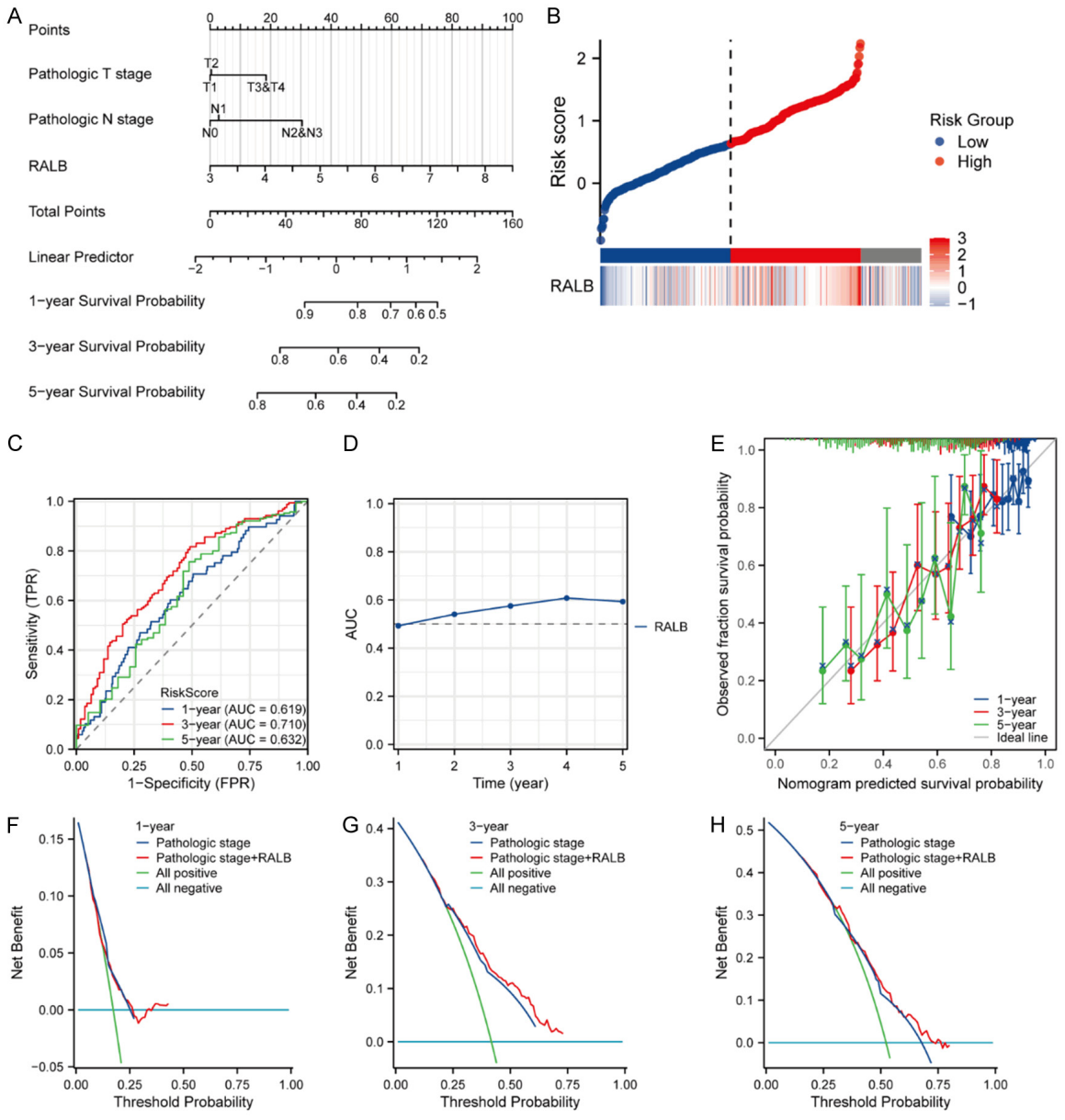

Figure 3. The value of RALB as a prognostic marker in HNSCC. (A) The nomogram based on COX multivariate hazard regression was used to predict the 1-, 3-, and 5-year survival of HNSCC patients. (B) Risk factor visualization based on nomogram-calculated risk scores and RALB expression levels. (C) Time-dependent ROC curves were used to assess the sensitivity of the nomogram at 1, 3, and 5 years. (D) Time-dependent AUC curve, according to the area under the time-dependent ROC curve, was used to evaluate the sensitivity of the nomogram at different time points. (E) Calibration curves for predicting patient survival at each time point. (F-H) DCA curves for evaluating the benefits of introducing RALB into the HNSCC prognosis prediction system at 1 (F), 3 (G), and 5 (H) years.

prediction system yearly for 1-5 years, which further confirmed its reliability (**Figure 3D**). Furthermore, we utilized the a DCA curve to compare he prognostic value of the RALB expression level in HNSCC patients with that of the pathological grade alone. The findings indicated that adding the RALB to HNSCC prognostic evaluation begins to yield significant observations after three years (**Figure 3F-H**).

Potential biological functions of RALB in HNSCC

RALB has been implicated in the malignant behavior of various tumors, indicating its potential role in regulating the biological behavior of HNSCC cells. To investigate this possibility, we categorized HNSCC samples from The TCGA into two groups according to the RALB mRNA level: RALB high vs. low expression. DEG analysis revealed that 91 genes were upregulated in the RALB high expression group, as demonstrated by a volcano plot (**Figure 4A**). KEGG/GO analysis of DEGs indicated that metabolism-related gene pathways, including the "xenobiotic metabolic process", "fatty acid metabolic process", "xenobiotic glucuronidation", "NAD+ activity", "NADP+ activity", and "drug metabolism", were more active in the RALB high expression group. Some carcinogenesis pathways such as the "chemical carcinogenesis - receptor activation" and "chemical carcinogenesis - DNA adducts" were also observed (**Figure 4B**). Moreover, the behavioral pathways related to tissue differentiation exhibited relatively negative characteristics, encompassing processes such as "keratinocyte differentiation", "intermediate filament organization", "structural constituents of skin epidermis", and "primary immunodeficiency" (**Figure 4C**). This finding suggests that tumor tissues exhibiting elevated levels of RAS exhibit a decreased degree of cellular differentiation, rendering them more malignant.

RALB enhances the proliferation, migration, and invasion capabilities of HNSCC cells

To further investigate the role of RALB in HNSCC, we designed three specific small interfering RNAs (siRNAs) targeting RALB to downregulate its expression (Figure S1). Subsequently, we transfected these siRNAs into HN-1 and HN-5 cells and assessed their efficacy at the RALB mRNA level. The RT-qPCR results revealed that all three siRNAs successfully reduced RALB mRNA levels; however, given its superior knockdown efficiency, we selected siRNA-2 for further functional assays (average knockdown of 35%) (Figure S1). We used functional experiments to detect the effect of changes in the expression level of RALB on the cellular functions of HNSCC related to the malignant phenotype. Notably, the EdU assays demonstrated a significant reduction in proliferation capacity among HNSCC cells transfected with siRNA-2 (**Figure 5A-C**). Wound healing assays revealed that within the same 24 h, the scratch healing distance of HNSCC cells in the si-RALB group was significantly shorter than that in the control group (**Figure 5D-F**). Transwell assays revealed a marked decrease in invasive ability among HNSCC cells upon downregulating RALB expression (**Figure 5G-I**). Our functional assays demonstrated that RALB enhances the proliferation, migration, and invasion capabilities of HNSCC cells in vitro, whereas its depletion effectively impedes disease progression.

RALB levels correlate with immune infiltration in HNSCC

Since immunotherapy plays a crucial role in treating cancer in contemporary medicine, we analyzed the correlation between the RALB expression and immune infiltration levels, as well as the immune score. The GSEA-based single sample gene set enrichment analysis (ssGSEA) algorithm was used to assess the degree of infiltration of diverse immune cells and their correlation with RALB expression in HNSCC samples from the TCGA. Results revealed that T helper (Th) 2 cells, neutrophils, eosinophils, macrophages, central memory T cells (Tcm), and gamma delta T cells (Tgd) cells positively correlate with RALB expression level. Conversely, dendritic cells (DCs), cytotoxic cells, CD8+ T cells, natural killer cells (NK cells), CD56dim cells, T cells, B cells, regulatory T cells (Tregs) (**Figure 6A**). Effector memory T cells (Tems) were negatively correlated with the RALB expression level (**Figure 6A**). The ESTIMATES algorithm was used, and the results indicated that the stromal score did not correlate with RALB, while the immune score was negatively associated with the RALB expression level (**Figure 6B**). Additionally, we used the TIMER tool to evaluate immune cell infiltration

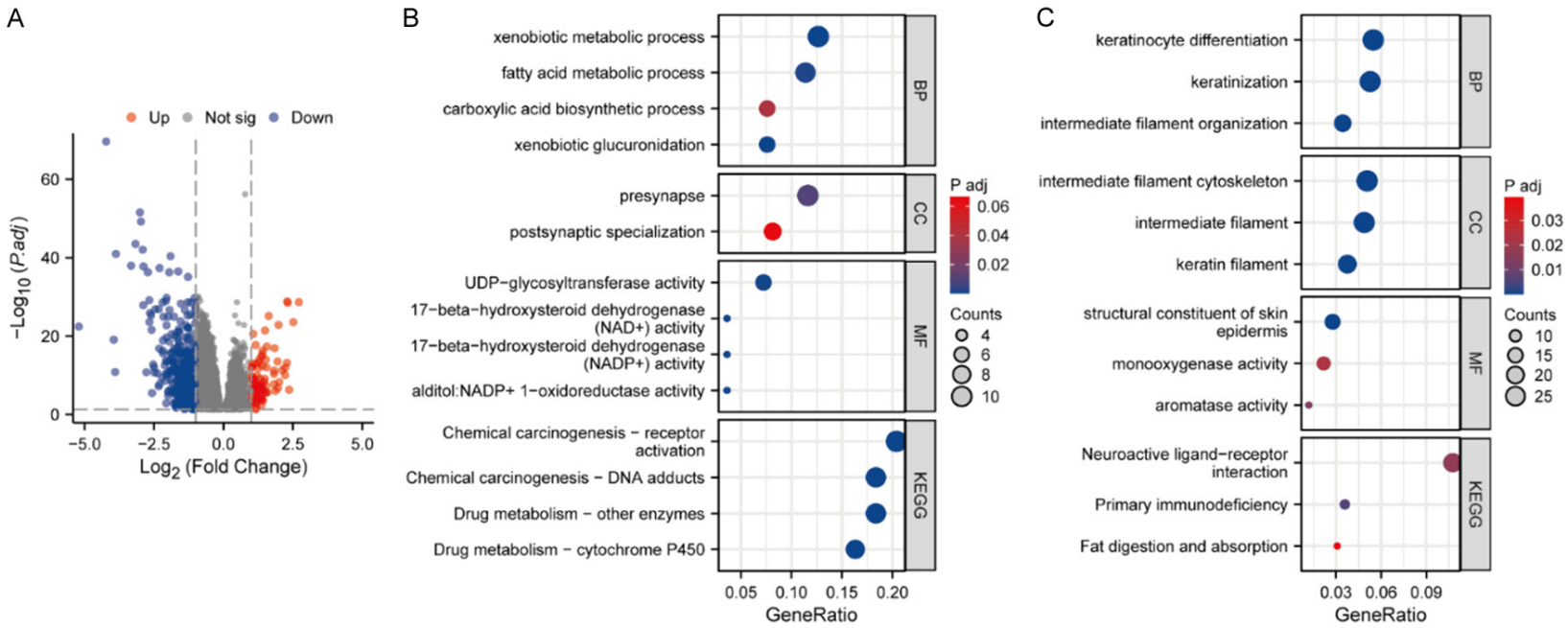

Figure 4. Potential biological function of RALB in HNSCC. (A) Volcano plots of Differential Expression Genes (DEGs) between RALB high expression group and RALB low expression group in HNSCC samples from TCGA. Gene enrichment analyses were performed based on the (B) 91 upregulated DEGs and (C) 596 downregulated DEGs. MF, Molecular Function; BP, Biological Process; CC, Cellular Components; KEGG, Kyoto Encyclopedia of Genes and Genomes.

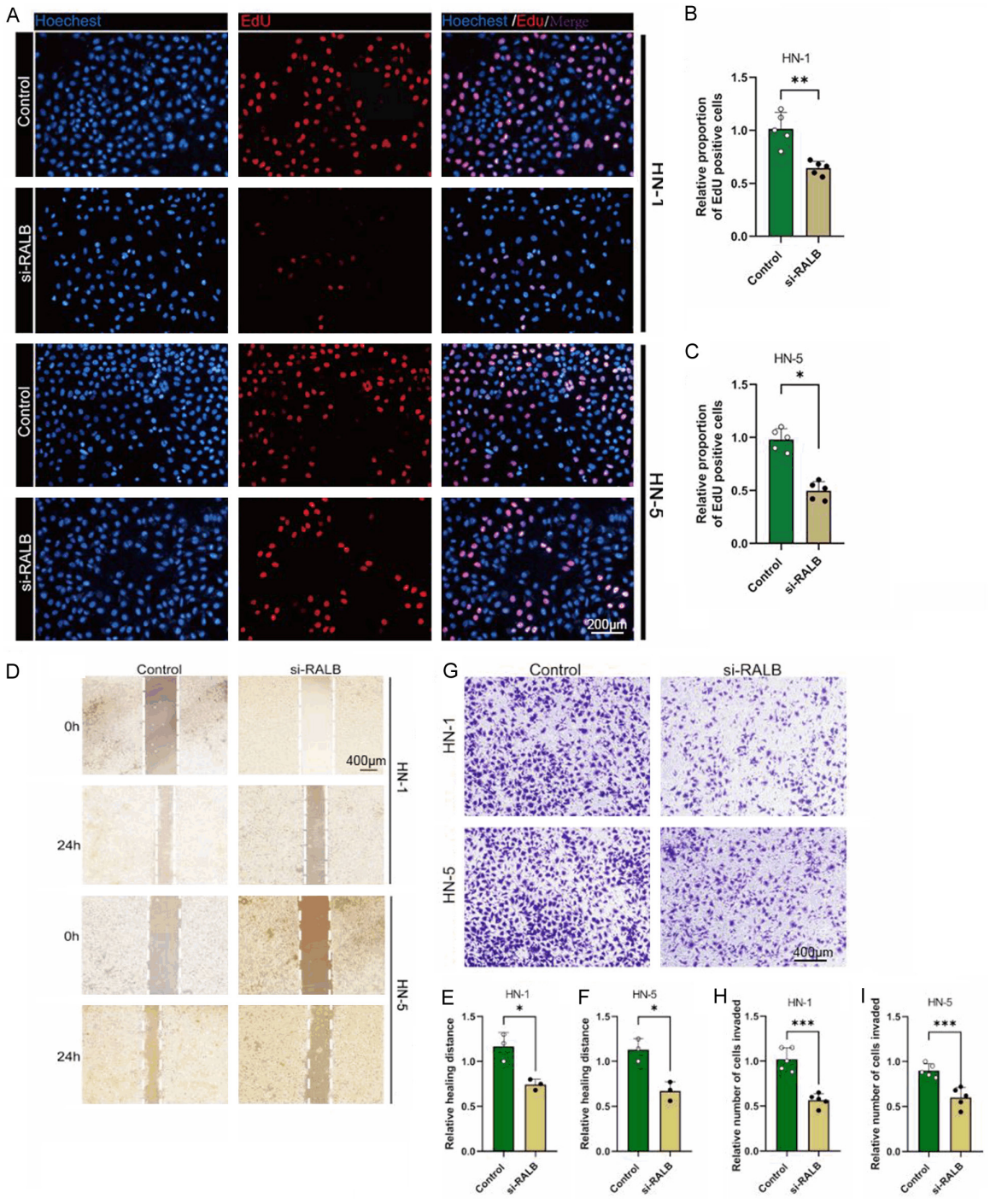

Figure 5. RALB enhances the proliferation, migration, and invasion of HNSCC cells. (A-C) Using EdU assay to detect the intervention ability of RALB siRNA on the proliferation of HN-1 and HN-5 cells. (A) representative images of EdU assay and (B and C) quantitative statistics, Nuclei stained with DAPI (blue); Proliferating cells stained with EDU (red). (D-F) The effect of si-RALB on the migration ability of HN-1 and HN-5 cells as detected by scratch healing assay; the white line marked the edge of the cell colony (D), and the relative healing distance was quantified (E and F), *, P<0.05. (G-I) The matrigel invasion assay was used to evaluate the effect of si-RALB on the invasion ability of HN-1 and HN-5 cells. The cells that passed through the matrigel and reached the lower surface of the transwell were stained purple with crystal violet dye (G), and the number of relative invasive cells was quantified by statistics (H and I). *, *P*<0.05; **, *P*<0.01; ***, *P*<0.001.

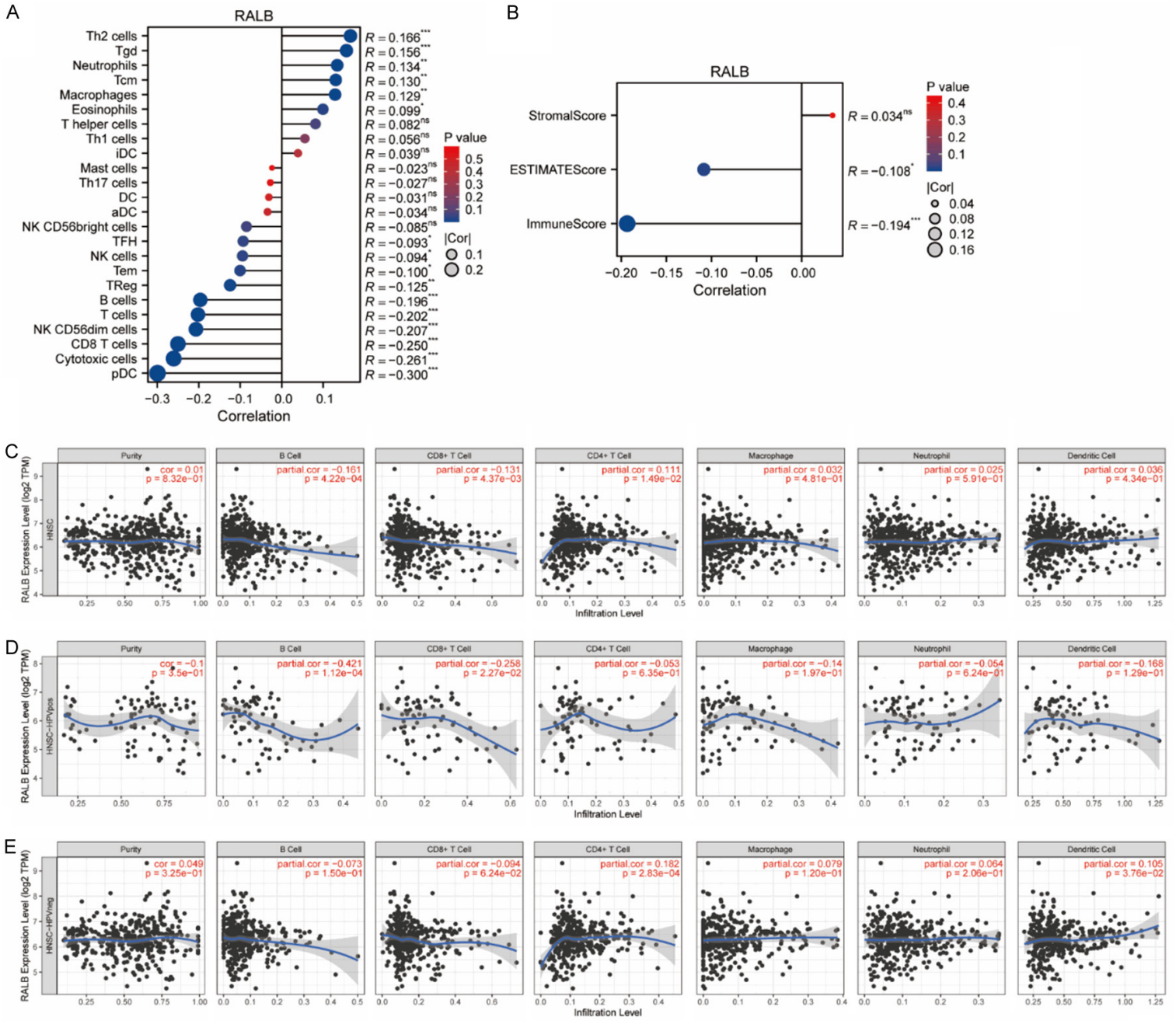
A
RALB
Th2 cells
Tgd
Neutrophils
Tcm
Macrophages
Eosinophils
T helper cells
Th1 cells
iDC
Mast cells
Th17 cells
DC
aDC
NK CD56bright cells
TFH
NK cells
Tem
TReg
B cells
T cells
NK CD56dim cells
CD8 T cells
Cytotoxic cells
pDC
R = 0.166***
R = 0.156***
R = 0.134**
R = 0.130**
R = 0.129**
R = 0.099*
R = 0.082ns
R = 0.056ns
R = 0.039ns
R = −0.023ns
R = −0.027ns
R = −0.031ns
R = −0.034ns
R = −0.085ns
R = −0.093*
R = −0.094*
R = −0.100*
R = −0.125**
R = −0.196***
R = −0.202***
R = −0.207***
R = −0.250***
R = −0.261***
R = −0.300***
P value
0.5
0.4
0.3
0.2
0.1
|Cor|
0.1
0.2
−0.3 −0.2 −0.1 0.0 0.1
Correlation
B
RALB
StromalScore
ESTIMATEScore
ImmuneScore
R = 0.034ns
R = −0.108*
R = −0.194***
P value
0.4
0.3
0.2
0.1
|Cor|
0.04
0.08
0.12
0.16
−0.20 −0.15 −0.10 −0.05 0.00
Correlation
C
Purity
cor = 0.01
p = 8.32e−01
B Cell
partial.cor = −0.161
p = 4.22e−04
CD8+ T Cell
partial.cor = −0.131
p = 4.37e−03
CD4+ T Cell
partial.cor = 0.111
p = 1.49e−02
Macrophage
partial.cor = 0.032
p = 4.81e−01
Neutrophil
partial.cor = 0.025
p = 5.91e−01
Dendritic Cell
partial.cor = 0.036
p = 4.34e−01
RALB Expression Level (log2 TPM)
HNSC
Infiltration Level
D
Purity
cor = −0.1
p = 3.5e−01
B Cell
partial.cor = −0.421
p = 1.12e−04
CD8+ T Cell
partial.cor = −0.258
p = 2.27e−02
CD4+ T Cell
partial.cor = −0.053
p = 6.35e−01
Macrophage
partial.cor = −0.14
p = 1.97e−01
Neutrophil
partial.cor = −0.054
p = 6.24e−01
Dendritic Cell
partial.cor = −0.168
p = 1.29e−01
RALB Expression Level (log2 TPM)
HNSC−HPVpos
Infiltration Level
E
Purity
cor = 0.049
p = 3.25e−01
B Cell
partial.cor = −0.073
p = 1.50e−01
CD8+ T Cell
partial.cor = −0.094
p = 6.24e−02
CD4+ T Cell
partial.cor = 0.182
p = 2.83e−04
Macrophage
partial.cor = 0.079
p = 1.20e−01
Neutrophil
partial.cor = 0.064
p = 2.06e−01
Dendritic Cell
partial.cor = 0.105
p = 3.76e−02
RALB Expression Level (log2 TPM)
HNSC−HPVneg
Infiltration Level

Figure 6. Correlation between RALB and degree of immune cell infiltration in HNSCC. A. The lollipop plot is based on the correlation between RALB and immune cell abundance in HNSCC, which was obtained from ssGSEA analysis. B. Lollipop plot based on the correlation between RALB and immune-related scores obtained from ESTIMATES analysis. C-E. Correlation between RALB and immune cell infiltration in HNSCC samples from TCGA obtained from TIMER. C. Whole HNSCC samples. D. HPV-positive HNSCC samples. E. HPV-negative HNSCC samples. ns, no significance; *, $P<0.05$; **, $P<0.01$; ***, $P<0.001$.

in HNSCC tissues relative to that of RALB, in HPV-positive and HPV-negative samples. Consistent with the ssGSEA results, B cells, CD8 T cells, CD4 T cells, macrophages, neutrophils, and DCs were correlated with the RALB expression levels (**Figure 6C**). However, these correlations differed between HPV-positive and HPV-negative HNSCC tissues. Specifically, in HPV-positive HNSCC tissues. Only B cells and CD8+ T cells exhibited a significant correlation with the RALB expression level (**Figure 6D**), whereas in HPV-negative HNSCC tissues, CD4+ T cells, CD8+ T cells, and DCs were significantly correlated with the RALB level (**Figure 6E**), indicating a noteworthy synergy among these cell types.

Discussion

RAL-GTPases can play redundant, compensatory, or divergent roles in a cancer-dependent or even cell line-dependent manner. RALB exhibits diverse functions as reported in cancer studies, but little is known about the role of RALB in head and neck cancer [18]. Only one previous study on laryngeal carcinoma cells attempted to target RALB as a therapeutic intervention by inducing its degradation through dihydroartemisinin in an *in vitro*, which resulted in the induction of autophagy [11]. However, the expression pattern of RALB in the tissues of HNSCC patients and its malignant phenotype in HNSCC cells are largely unknown. Therefore, in this study, we investigated whether the dysregulation of RALB in HNSCC is associated with patient survival and whether the inhibition of RALB is associated with the malignant phenotype of HNSCC cells *in vitro*.

Our study revealed a high expression level of RALB in HNSCC tissues and a significant positive correlation between the RALB expression and NRAS/KRAS expression. RALB has been reported to be significantly upregulated in bladder, colorectal, and pancreatic cancers patients relative to that in normal controls [12, 13, 19]. Knockdown of RALB by shRNA in colorectal cancer cells significantly increases anchorage-independent growth regardless of KRAS mutation status [20]. Whether RALB signaling downstream of the RAS plays a role in HNSCC needs to be further studied. It was observed that high RALB expression is associated with poor prognosis in HNSCC patients, in agreement with the results in colorectal cancer patients [8]. Furthermore, we found that high RALB expression is an independent prognostic risk factor for HNSCC patients, indicating that its upregulation is a valuable risk factor for HNSCC progression.

We examined the effect of siRNA-mediated silencing of RALB on the malignant phenotype of HNSCC cells and found that the inhibition of RALB could effectively impede the proliferation, invasion, and migration capabilities of HNSCC cells by downregulating the malignant phenotype, by approximately 50%. RALB has been found to be required for the migrating bladder cancer cells in studies employing RALB-specific siRNAs [21]. The phosphorylation of RALB is required for the tumor growth, metastasis, and migration of bladder cancer cells. Cell migration in lung cancer appears to be a RALB driven phenotype, and knockdown of RALB reduces the spontaneous lung metastasis of 4T1 cells [22]. RALB lysine fatty acid acetylation has been found to be required for proper cell migration of lung cancer cells [23]. More functional and *in vivo* experiments are warranted to confirm the potential of RALB as a novel therapeutic target and treatment strategy for HNSCC.

Interestingly, our study revealed a correlation between RALB expression and the degree of immune infiltration in HNSCC, particularly to CD8+ T cells, CD4+ T cells, and NK cells in HPV-positive HNSCC tissue samples. The fundamental principle of immunotherapy involves activating the immune system, which is suppressed by various factors in cancer patients to eliminate malignant cells. There have also been studies linking RAL GTPases with tumor immunotherapy that systematically identified the expression levels of RALA across cancers and its association with immune cells. The aforementioned studies revealed a significant

correlation between the expression level of RALA and the infiltration level of B cells and macrophages, as well as with the expression levels of multiple immune checkpoints [24]. However, research on the relationship between RALB and tumor immunotherapy is still limited. Specifically, RALB is required to suppress apoptotic checkpoint activation [25, 26]. The RALB pathway inhibits apoptosis in tumor cells and stimulates an innate immune response in nontumorigenic cells [25]. Ubiquitylation within the effector-binding domain provides a switch for the dual functions of RALB in autophagy and innate immune responses [27]. By establishing a link between RALB and T cell-mediated immune responses, it may help to identify a subset of HNSCC patients who are more responsive to immunotherapy or to develop novel adjuvant therapeutic targets and strategies for HNSCC.

In summary, this study revealed that RALB expression is elevated in HNSCC and is significantly associated with its poor prognosis. The effective targeting of RALB impedes the malignant phenotype of HNSCC cells. Furthermore, we provided insight into the relationship between RALB and T cell-mediated immune responses. Further RALB-associated studies may provide new insights into an innovative strategy for HNSCC immunotherapy.

Acknowledgements

This study was funded by the National Natural Science Foundation of China (81402236, 81772887), Jiangsu Provincial Medical Innovation Team (CXTDA2017036), the Priority Academic Program Development of Jiangsu Higher Education Institutions (PAPD, 2018-87), Jiangsu Provincial Medical Youth Talent (QNRC2016854) and Natural Science Foundation of Jiangsu Province of China (BK20171488).

Disclosure of conflict of interest

None.

Abbreviations

HNSCC, head and neck squamous cell carcinoma; RALB, RAS-like oncogene B; RAL GTPase, RAS-like GTPase; DEGs, differential expression genes; TCGA, The Cancer Genome Atlas; GteX, Genotype-Tissue Expression; ssGSEA, single sample gene set enrichment analysis; OS, overall survival; DSS, disease-specific survival; RFI, recurrence-free interval; NAD, nicotinamide adenine dinucleotide; NADP, nicotinamide adenine dinucleotide phosphate; Th, T helper; Tcm, central memory T cells; Tgd, gamma delta T cells; NK, natural killer; Treg, regulatory T cells; Tem, effector memory T cells.

Address correspondence to: Xiao-Meng Song, Department of Oral and Maxillofacial Surgery, Affiliated Hospital of Stomatology, Nanjing Medical University, No. 136 Hanzhong Road, Nanjing 210019, Jiangsu, China. E-mail: xiaomengsong@njmu.edu.cn

References

[1] Verdonck-de Leeuw I, Dawson C, Licitra L, Eriksen JG, Hosal S, Singer S, Laverty DP, Golusinski W, Machczynski P, Varges Gomes A, Girvalaki C, Simon C and Leemans CR. European Head and Neck Society recommendations for head and neck cancer survivorship care. Oral Oncol 2022; 133: 106047.

[2] Cai XJ, Zhang HY, Zhang JY and Li TJ. Bibliometric analysis of immunotherapy for head and neck squamous cell carcinoma. J Dent Sci 2023; 18: 872-882.

[3] Ran QC, Long SR, Ye Y, Xie C, XuXiao ZL, Liu YS, Pang HX, Sunchuri D, Teng NC and Guo ZL. Mining TCGA database for prognostic genes in head and neck squamous cell carcinoma microenvironment. J Dent Sci 2021; 16: 661-667.

[4] Gu Y, Tang S, Wang Z, Cai L, Shen Y and Zhou Y. Identification of key miRNAs and targeted genes involved in the progression of oral squamous cell carcinoma. J Dent Sci 2022; 17: 666-676.

[5] Tian X, Shi C, Liu S, Zhao C, Wang X and Cao Y. Methylation related genes are associated with prognosis of patients with head and neck squamous cell carcinoma via altering tumor immune microenvironment. J Dent Sci 2023; 18: 57-64.

[6] Sun L, Xing G, Wang W, Ma X and Bu X. Proliferation-associated 2G4 P48 is stabilized by malignant T-cell amplified sequence 1 and promotes the proliferation of head and neck squamous cell carcinoma. J Dent Sci 2023; 18: 1588-1597.

[7] Zago G, Veith I, Singh MK, Fuhrmann L, De Beco S, Remorino A, Takaoka S, Palmeri M, Berger F, Brandon N, El Marjou A, Vincent-Salomon A, Camonis J, Coppey M and Parrini MC. RalB directly triggers invasion downstream

Ras by mobilizing the Wave complex. Elife 2018; 7: e40474.
[8] Martin TD and Der CJ. Differential involvement of RalA and RalB in colorectal cancer. Small GTPases 2012; 3: 126-130.
[9] Richardson DS, Spehar JM, Han DT, Chakravarthy PA and Sizemore ST. The RAL enigma: distinct roles of RALA and RALB in cancer. Cells 2022; 11: 1645.
[10] Pomeroy EJ and Eckfeldt CE. Targeting Ras signaling in AML: RALB is a small GTPase with big potential. Small GTPases 2020; 11: 39-44.
[11] Shi X, Li S, Wang L, Li H, Li Z, Wang W, Bai J, Sun Y, Li J and Li X. RalB degradation by dihydroartemisinin induces autophagy and IFI16/caspase-1 inflammasome depression in the human laryngeal squamous cell carcinoma. Chin Med 2020; 15: 64.
[12] Smith SC, Oxford G, Baras AS, Owens C, Havaleshko D, Brautigan DL, Safo MK and Theodorescu D. Expression of ral GTPases, their effectors, and activators in human bladder cancer. Clin Cancer Res 2007; 13: 3803-3813.
[13] Martin TD, Samuel JC, Routh ED, Der CJ and Yeh JJ. Activation and involvement of Ral GTPases in colorectal cancer. Cancer Res 2011; 71: 206-215.
[14] Fan G, Zhu Y, Zhu H, Yu L, Wang Z, Zhai C, Zhou G, Zhao J and Wang Y. Identification of RALA as a therapeutic target and prognostic predictor of osteosarcoma. Biomed Res Int 2023; 2023: 1150768.
[15] Guin S and Theodorescu D. The RAS-RAL axis in cancer: evidence for mutation-specific selectivity in non-small cell lung cancer. Acta Pharmacol Sin 2015; 36: 291-297.
[16] Yan C and Theodorescu D. RAL GTPases: biology and potential as therapeutic targets in cancer. Pharmacol Rev 2018; 70: 1-11.
[17] Li T, Fu J, Zeng Z, Cohen D, Li J, Chen Q, Li B and Liu XS. TIMER2.0 for analysis of tumor-infiltrating immune cells. Nucleic Acids Res 2020; 48: W509-W514.
[18] Biondini M, Duclos G, Meyer-Schaller N, Silberzan P, Camonis J and Parrini MC. RalB regulates contractility-driven cancer dissemination upon TGFbeta stimulation via the RhoGEF GEF-H1. Sci Rep 2015; 5: 11759.
[19] Beel S, Kolloch L, Apken LH, Jurgens L, Bolle A, Sudhof N, Ghosh S, Wardelmann E, Meisterernst M, Steinestel K and Oeckinghaus A. kappaB-Ras and Ral GTPases regulate acinar to ductal metaplasia during pancreatic adenocarcinoma development and pancreatitis. Nat Commun 2020; 11: 3409.
[20] Khawaja H, Campbell A, Roberts JZ, Javadi A, O'Reilly P, McArt D, Allen WL, Majkut J, Rehm M, Bardelli A, Di Nicolantonio F, Scott CJ, Kennedy R, Vitale N, Harrison T, Sansom OJ, Longley DB, Evergren E and Van Schaeybroeck S. RALB GTPase: a critical regulator of DR5 expression and TRAIL sensitivity in KRAS mutant colorectal cancer. Cell Death Dis 2020; 11: 930.
[21] Wang H, Owens C, Chandra N, Conaway MR, Brautigan DL and Theodorescu D. Phosphorylation of RalB is important for bladder cancer cell growth and metastasis. Cancer Res 2010; 70: 8760-8769.
[22] Hyenne V, Apaydin A, Rodriguez D, Spiegelhalter C, Hoff-Yoessle S, Diem M, Tak S, Lefebvre O, Schwab Y, Goetz JG and Labouesse M. RAL-1 controls multivesicular body biogenesis and exosome secretion. J Cell Biol 2015; 211: 27-37.
[23] Spiegelman NA, Zhang X, Jing H, Cao J, Kotliar IB, Aramsangtienchai P, Wang M, Tong Z, Rosch KM and Lin H. SIRT2 and lysine fatty acylation regulate the activity of RalB and cell migration. ACS Chem Biol 2019; 14: 2014-2023.
[24] Jin H, Qin S, He J, Xiao J, Li Q, Mao Y and Zhao L. Systematic pan-cancer analysis identifies RALA as a tumor targeting immune therapeutic and prognostic marker. Front Immunol 2022; 13: 1046044.
[25] Chien Y, Kim S, Bumeister R, Loo YM, Kwon SW, Johnson CL, Balakireva MG, Romeo Y, Kopelovich L, Gale M Jr, Yeaman C, Camonis JH, Zhao Y and White MA. RalB GTPase-mediated activation of the IkappaB family kinase TBK1 couples innate immune signaling to tumor cell survival. Cell 2006; 127: 157-170.
[26] Mantovani A and Balkwill F. RalB signaling: a bridge between inflammation and cancer. Cell 2006; 127: 42-44.
[27] Simicek M, Lievens S, Laga M, Guzenko D, Aushev VN, Kalev P, Baietti MF, Strelkov SV, Gevaert K, Tavernier J and Sablina AA. The deubiquitylase USP33 discriminates between RALB functions in autophagy and innate immune response. Nat Cell Biol 2013; 15: 1220-1230.

Table S1. siRNA and control plasmids sequences in this study

Primer	Sequence	Sequences (5'-3')
siRNA-1	Sense Sequence	GACCUAAUGAGAGAAAUCAGAACAA
siRNA-1	Antisense Sequence	UUGUUCUGAUUUCUCUCAUUAGGUC
siRNA-1-control	Sense Sequence	GACUAAGAGAGAUAAGACAACUCAA
siRNA-1-control	Antisense Sequence	UUGAGUUGUCUUAUCUCUCUUAGUC
siRNA-2	Sense Sequence	GAAAUCAGAACAAAGAAGAUGUCAG
siRNA-2	Antisense Sequence	CUGACAUCUUCUUUGUUCUGAUUUC
siRNA-2-control	Sense Sequence	GAAAGACAACAAAGAGUAGUUACAG
siRNA-2-control	Antisense Sequence	CUGUAACUACUCUUUGUUGUCUUUC
siRNA-3	Sense Sequence	GAGAGAAAUCAGAACAAAGAAGAUG
siRNA-3	Antisense Sequence	CAUCUUCUUUGUUCUGAUUUCUCUC
siRNA-3-control	Sense Sequence	GAGAAUAACAGCAAAGAAAGGAAUG
siRNA-3-control	Antisense Sequence	CAUUCCUUUCUUUGCUGUUAUUCUC

Table S2. Primer sequences for qRT-PCR in this study

Primer	Sequences (5'-3')
hsa-RALB-F	ATGGCTGCAAATAAGCCCAAG
hsa-RALB-R	TGTCTGCTTTGGTAGGCTCATA
hsa-GAPDH-F	CGAGCCACATCGCTCAGACA
hsa-GAPDH-R	GTGGTGAAGACGCCAGTGGA

Table S3. Clinicopathologic features of HNSCC patients downloaded from TCGA based on RALB expression

Characteristics	Low expression of RALB	High expression of RALB	*P* value
n	252	252	
T stage, n (%)			0.051
T1	24 (5.4%)	21 (4.7%)	
T2	75 (16.7%)	60 (13.4%)	
T3	36 (8%)	60 (13.4%)	
T4	83 (18.5%)	89 (19.9%)	
N stage, n (%)			0.831
N0	83 (20.2%)	88 (21.4%)	
N1	34 (8.3%)	32 (7.8%)	
N2&N3	82 (20%)	92 (22.4%)	
M stage, n (%)			0.460
M0	102 (54%)	86 (45.5%)	
M1	0 (0%)	1 (0.5%)	
Pathologic stage, n (%)			0.812
Stage I	14 (3.2%)	11 (2.5%)	
Stage II	36 (8.3%)	34 (7.8%)	
Stage III	37 (8.5%)	42 (9.6%)	
Stage IV	125 (28.7%)	137 (31.4%)	
Age, n (%)			0.562
≤60	120 (23.9%)	127 (25.2%)	
>60	131 (26%)	125 (24.9%)	
Gender, n (%)			0.687
Female	69 (13.7%)	65 (12.9%)	
Male	183 (36.3%)	187 (37.1%)	
Histologic grade, n (%)			0.215
G1	34 (7%)	28 (5.8%)	
G2	140 (28.9%)	161 (33.3%)	
G3	68 (14%)	51 (10.5%)	
G4	1 (0.2%)	1 (0.2%)	
OS event, n (%)			<0.001
Alive	162 (32.1%)	124 (24.6%)	
Dead	90 (17.9%)	128 (25.4%)	
DSS event, n (%)			<0.001
No	191 (39.9%)	158 (33%)	
Yes	49 (10.2%)	81 (16.9%)	
PFS event, n (%)			<0.001
No	174 (34.5%)	136 (27%)	
Yes	78 (15.5%)	116 (23%)	

OS, overall survival; DSS, disease specific survival; PFS, progression free survival.

Table S4. Clinicopathologic features of 90 HNSCC patients clinical samples based on RALB expression

Characteristics	Amount	High expression of RALB	Low expression of RALB	*P* value
Age				0.6053
<60	61	33	28	
≥60	29	14	15	
Gender				0.3762
Male	59	21	38	
Female	31	14	17	
Smoke				0.1384
Yes	72	30	42	
No	18	11	7	
Alcohol				0.1488
Yes	36	16	20	
No	54	27	27	
Histological differentiation				0.000
Highly	62	18	44	
Moderately to poorly	28	22	6	
TNM stage				0.002
I/II	47	20	27	
III/IV	43	32	11	
Lymph node metastasis				0.000
N0	43	15	28	
N+	47	41	6	

Table S5. Univariate and multivariate COX hazard ratio regression

Characteristics	Total (N)	Univariate analysis		Multivariate analysis	
		Hazard ratio (95% CI)	*P* value	Hazard ratio (95% CI)	*P* value
T stage	447				
T1	45	Reference		Reference	
T2	134	1.341 (0.694-2.590)	0.382	1.096 (0.317-3.793)	0.885
T3	96	2.592 (1.349-4.984)	0.004	1.657 (0.493-5.567)	0.414
T4	172	2.347 (1.250-4.407)	0.008	1.838 (0.530-6.379)	0.338
N stage	410				
N0	170	Reference		Reference	
N1	66	0.957 (0.563-1.624)	0.870	0.933 (0.500-1.742)	0.829
N2&N3	174	2.269 (1.617-3.183)	<0.001	2.148 (1.335-3.453)	0.002
Pathologic stage	435				
Stage I	25	Reference		Reference	
Stage II	69	1.919 (0.667-5.521)	0.227	1.078 (0.180-6.462)	0.934
Stage III	79	2.193 (0.768-6.259)	0.142	1.683 (0.313-9.051)	0.544
Stage IV	262	3.465 (1.281-9.375)	0.014	1.349 (0.236-7.707)	0.737
Age	503				
≤60	247	Reference		Reference	
>60	256	1.262 (0.964-1.653)	0.090	1.320 (0.954-1.827)	0.094
Gender	503				
Female	134	Reference		Reference	
Male	369	0.760 (0.571-1.012)	0.061	0.704 (0.496-0.998)	0.048
RALB	503				
Low	251	Reference		Reference	
High	252	1.436 (1.095-1.882)	0.009	1.506 (1.088-2.086)	0.014

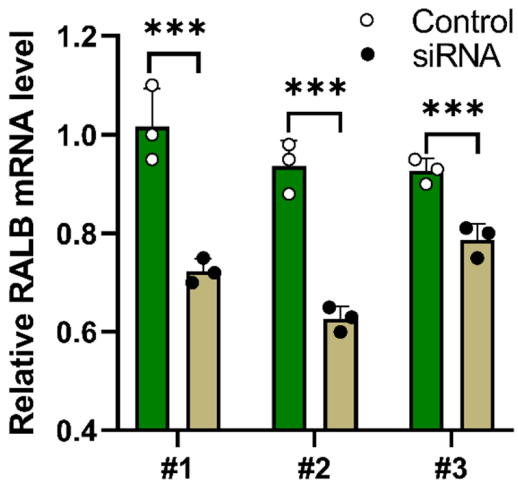

Figure S1. Knockdown ability of three siRNAs (#1, #2 and #3) for RALB mRNA in HN-1 cells was detected by RT-qPCR.